THE JOURNAL OF BIOLOGICAL CHEMISTRY VOL. 291, NO. 23, pp. 12184–12194, June 3, 2016

Smad2/3 Proteins Are Required for Immobilization-induced Skeletal Muscle Atrophy*

Received for publication, July 21, 2015, and in revised form, March 24, 2016 Published, JBC Papers in Press, April 15, 2016, DOI 10.1074/jbc.M115.680579

Toshimi Tando[‡], Akiyoshi Hirayama[§], Mitsuru Furukawa[‡], Yuiko Sato[‡¶], Tami Kobayashi[‡¶], Atsushi Funayama[‡], Arihiko Kanaji[‡], Wu Hao[‡], Ryuichi Watanabe[‡], Mayu Morita[‖], Takatsugu Oike[‡], Kana Miyamoto[‡], Tomoyoshi Soga[§], Masatoshi Nomura[**], Akihiko Yoshimura[‡‡], Masaru Tomita[§], Morio Matsumoto[‡], Masaya Nakamura[‡], Yoshiaki Toyama[‡], and Takeshi Miyamoto[‡1]

From the Departments of [‡]Orthopedic Surgery, [¶]Musculoskeletal Reconstruction and Regeneration Surgery, [‡‡]Immunology, and [‖]Dentistry and Oral Surgery, Keio University School of Medicine, 35 Shinano-machi, Shinjuku-ku, Tokyo 160-8582, the [§]Institute for Advanced Biosciences, Keio University, 246-2 Mizukami, Kakuganji, Tsuruoka, Yamagata 997-0052, and the [**]Department of Medicine and Bioregulatory Science, Graduate School of Medical Science, Kyushu University, Maidashi 3-1-1, Higashi Ward, Fukuoka 812-8582, Japan

Skeletal muscle atrophy promotes muscle weakness, limiting activities of daily living. However, mechanisms underlying atrophy remain unclear. Here, we show that skeletal muscle immobilization elevates Smad2/3 protein but not mRNA levels in muscle, promoting atrophy. Furthermore, we demonstrate that myostatin, which negatively regulates muscle hypertrophy, is dispensable for denervation-induced muscle atrophy and Smad2/3 protein accumulation. Moreover, muscle-specific Smad2/3-deficient mice exhibited significant resistance to denervation-induced muscle atrophy. In addition, expression of the atrogenes *Atrogin-1* and *MuRF1,* which underlie muscle atrophy, did not increase in muscles of Smad2/3-deficient mice following denervation. We also demonstrate that serum starvation promotes Smad2/3 protein accumulation in C2C12 myogenic cells, an *in vitro* muscle atrophy model, an effect inhibited by IGF1 treatment. *In vivo*, we observed IGF1 receptor deactivation in immobilized muscle, even in the presence of normal levels of circulating IGF1. Denervation-induced muscle atrophy was accompanied by reduced glucose intake and elevated levels of branched-chain amino acids, effects that were Smad2/3-dependent. Thus, muscle immobilization attenuates IGF1 signals at the receptor rather than the ligand level, leading to Smad2/3 protein accumulation, muscle atrophy, and accompanying metabolic changes.

Skeletal muscle homeostasis is maintained as a balance of anabolic and catabolic signals (1, 2). Insulin or growth hormone signals activate anabolic signals, whereas starvation, cachexia, prolonged disuse/unloading, or steroid treatment promotes muscle atrophy/wasting (3). Loss of muscle volume and power in the elderly frequently hampers activities of daily living, resulting in further muscle wasting and sarcopenia, which is characterized by further loss of muscle volume and power (4). These conditions in the elderly are also associated with falls, which cause fractures and potentially contribute to dementia. Defining mechanisms underlying muscle atrophy could encourage development of therapies to prevent these complications.

Younger individuals also can exhibit muscle atrophy from long bed rest, cachexia resulting from malignancies, high dose or long term steroid treatment, or even prolonged gravity-free conditions associated with space flight. Local atrophy can occur in muscles immobilized following injuries such as muscle/ligament/tendon ruptures or bone fracture. Local muscle atrophy, however, is usually not accompanied by systemic muscle atrophy and is instead thought to be driven by signals derived in the immobilized region.

Insulin/insulin-like growth factor 1 (IGF1) promotes anabolic signals in skeletal muscle via insulin receptor substrate 1 (IRS1) and PI3K, which in turn activates Akt, the mammalian target of rapamycin or p70 S6 kinase (p70S6K) (5, 6). In contrast, catabolic signals are transduced by Forkhead box O family members (FoxOs), muscle RING finger 1 (MuRF1, also called Trim63), Atrogin-1 (also called muscle atrophy F-box (MAFbx) or Fbxo32), or Cbl-b (7–10). Both MuRF1 and Atrogin-1 are RING-type ubiquitin ligases and FoxO targets (11, 12), and both regulate degradation of key muscle regulatory proteins such as MyoD, calcineurin, eIf3-f, myogenin, MyBP-C, MyLC, MyHC, and troponin 1 (13–19). In a denervation-induced muscle atrophy model (8), mice deficient in either MuRF1 or Atrogin-1 exhibit partial but significant muscle sparing relative to wild-type mice. The RING-type ubiquitin ligase Cbl-b, which is induced by muscle unloading, targets IRS1, a regulator of IGF1 signaling (10). Cbl-b-deficient mice are reportedly resistant to unloading-induced muscle atrophy (10). Stimulation by cytokines such as TNFα reportedly promotes muscle atrophy (20, 21). Myostatin (also called GDF8), which activates Smad2/3 via the activin receptor IIB (ActRIIB), reportedly inhibits muscle growth, and animal models and human subjects harboring myostatin mutations exhibit muscle hypertrophy (22–24). Thus, targeting the myostatin-ActRIIB pathway is considered one approach to block or prevent muscle wasting. Indeed, inhibiting myostatin-ActRIIB signaling reportedly prevents muscle wasting promoted by cancer in mice or seen in the Mdx mouse model of muscular dystrophy (25, 26). Clinical trials also

* This work was supported by a grant-in-aid for scientific research and in part by a grant from the Translational Research Network Program. The authors declare that they have no conflicts of interest with the contents of this article.
[1] To whom correspondence should be addressed. Tel.: 81-3-5363-3812; Fax: 81-3-3353-6597; E-mail: miyamoto@z5.keio.jp.

are now underway to test the effectiveness of blocking the myostatin-ActRIIB pathway in preventing muscle wasting (27). Finally, anabolic and catabolic signals interact (1, 2); IGF signals reportedly inhibit FoxOs, whereas Smads reportedly inhibit IGF1 signals (7, 12, 28).

Here, we report that Smad2/3 proteins but not mRNA accumulate in immobilized skeletal muscle following either denervation or limb fixation, an outcome required for immobilization-induced muscle atrophy, as lack of Smad2/3 completely abrogated the denervation-induced atrophy phenotype. Interestingly, lack of myostatin in adult mice did not prevent denervation-induced muscle atrophy, and Smad2/3 protein still accumulated in atrophic muscles of these mice. In normal cells, Smad2/3 proteins were continuously destabilized by IGF1 signaling, although muscle immobilization blocked IGF1-receptor activation, even in the presence of the IGF1 ligand *in vivo*. Finally, we show that muscle immobilization resulted in reduced glucose uptake but increased levels of branched-chain amino acids (BCAA)[2] in muscle.

Experimental Procedures

Mice—Mstnfl/fl mice carrying loxP-flanked Mstn alleles as well as Ckmm Cre mice were purchased from The Jackson Laboratory (Bar Harbor, ME). Inducible conditional Mstn knockout mice (Mx1 Cre; Mstnfl/fl) were generated by crossing Mstnfl/fl with Mx1 Cre transgenic mice. For denervation-induced muscle atrophy, 8-week-old mice were anesthetized, and then a 1-mm portion of sciatic nerve was removed to denervate the gastrocnemius muscle. For fixation-induced atrophy, 8-week-old mice were anesthetized, and the hindlimb was held in a fixed position by stapling (Autoclip, BD Biosciences). Thus, immobilization on one side was achieved by either denervation or fixation, and sham surgery was performed on the other hindlimb. Animals were maintained under specific pathogen-free conditions in animal facilities certified by the Keio University Animal Care Committee. Animal protocols were also approved by the committee.

Reagents—Recombinant mouse IGF1 was purchased from R&D Systems (Minneapolis, MN). LY294002, SIS3, and MG132 were obtained from Calbiochem, and U0126 was from Sigma.

Histology—Harvested muscles were fixed in 10% neutral-buffered formalin, embedded in paraffin, cut into 4-μm sections, and stained with hematoxylin and eosin. Fiber cross-sectional area (CSA) was analyzed in H&E-stained gastrocnemius muscle sections. For each muscle, CSA values were calculated by analyzing at least 1000 myofibers using BioRevo (Keyence, Osaka, Japan).

Real Time PCR Analysis—Total RNA was collected from gastrocnemius muscle cells using TRI Reagent (Molecular Research Center, Inc., Cincinnati, OH), and single-stranded complementary DNAs (cDNAs) were synthesized with reverse transcriptase (Clontech). Real time PCR was performed using SYBR Premix ExTaq II (Takara Bio Inc., Otsu, Shiga, Japan) with a DICE thermal cycler (Takara Bio Inc.), according to the manufacturer's instruction. β-Actin expression served as an internal control for real time PCR. Primer sequences were as follows: *Atrogin-1* forward, 5′-GAGACCATTCTACACTGGCAGCA-3′, and *Atrogin-1* reverse, 5′-GTCACTCAGCCTCTGCATGATGT-3′; *MuRF1* forward, 5′-ACCTGCTGGTGGAAAACATCATT-3′, and *MuRF1* reverse, 5′-AGGAGCAAGTAGGCACCTCACAC-3′; *Smad2* forward, 5′-CAGGACGGTTAGATGAGCTTGAGA-3′, and *Smad2* reverse, 5′-CCCACTGATCTACCGTATTTGCTG-3′; *Fbxo40* forward, 5′-ACCTCCTGGAAAGTCCACAATCAG-3′, and *Fbxo40* reverse, 5′-GACAGGTTTTCAGGTGCTCAGACA-3′; *Traf6* forward, 5′-TGCAAAAGATGGAACTGAGACATC-3′, and *Traf6* reverse, 5′-TGGGACAATCCTCAATAATGTGTG-3′; *Musa1/Fbxo30* forward, 5′-CTTCAGTCTCGTGGAATGGTAATCTT-3′, and *Musa1/Fbxo30* reverse, 5′-TGCAGTACTGAATCGCCATAC-3′; *Smart/Fbxo21* forward, 5′-TTTTTGAGGATGAGCTGGTGTGT-3′, and *Smart/Fbxo21* reverse, 5′-AGGAACGCCTTGAGGTTATTGAG-3′; *Fbxo31* forward, 5′-GCTCGAGGAACGAGGATTACCC-3′, and *Fbxo31* reverse, 5′-ATCCAAAGCGGTCCTCATCAAA-3′; and *ActB* forward, 5′-TGAGAGGGAAATCGTGCGTGAC-3′, and *ActB* reverse, 5′-AAGAAGGAAGGCTGGAAAAGAG-3′.

Western Blot Analysis—Harvested muscles were homogenized in RIPA buffer (1% Tween 20, 0.1% SDS, 150 nM NaCl, 10 mM Tris-HCl (pH 7.4), 0.25 mM phenylmethylsulfonyl fluoride, 10 μg/ml aprotinin, 10 μg/ml leupeptin, 1 mM Na_3VO_4, 5 mM NaF (Sigma)). Whole cell lysates were also prepared from C2C12 cells using RIPA buffer and collected after 10 min of centrifugation at 15,000 rpm at 4 °C. Equivalent amounts of protein were separated by SDS-PAGE and transferred to a PVDF membrane (Millipore Corp.). Proteins were detected using the following antibodies: anti-phospho-Smad2 (3101, Cell Signaling); anti-phospho-Smad3 (9520, Cell Signaling); anti-Smad2/3 (3102, Cell Signaling); anti-phospho-Smad1/5/8 (9511, Cell Signaling); anti-Smad1 (6944, Cell Signaling); anti-phospho-IGF1 receptor (3024, Cell Signaling); anti-IGF1 receptor (9750, Cell Signaling); anti-Akt (9272, Cell Signaling); anti-phospho Akt (4051, Cell Signaling); and anti-Actin (A2066, Sigma). Bands were quantified by National Institutes of Health imaging, as described (29, 30). For *in vitro* cell culture, C2C12 cells were cultured in growth medium (DMEM supplemented with 10% FCS, penicillin (50 units/ml), and streptomycin (100 μg/ml)) and maintained at 37 °C in humidified 5% CO_2 atmosphere. Cell differentiation was initiated by incubating 80% confluent cultures in differentiation medium (DMEM supplemented with 2% heat-inactivated horse serum) for 3 days to induce myotube formation. Then, medium was replaced by DMEM with or without 10% FCS representing respective non-starvation or starvation groups in the presence or absence of IGF1 (10 ng/ml), LY294002 (10 μM), SIS3 (10 μM), or MG132 (10 μM). After 6 or 24 h of incubation, cells were harvested for Western blotting or real time PCR, respectively. After 6 or 24 h of incubation, cells were harvested for Western analysis or real time PCR, respectively. Total RNAs were isolated using an RNeasy mini kit (Qiagen, Hilden, Germany). Bands were quantified as described previously (31).

ELISA—Serum IGF1 levels were measured by ELISA (R&D Systems, Minneapolis, MN) according to the manufacturer's instructions.

[2] The abbreviations used are: BCAA, branched-chain amino acid; CSA, cross-sectional area; DKO, double KO; cKO, conditional KO.

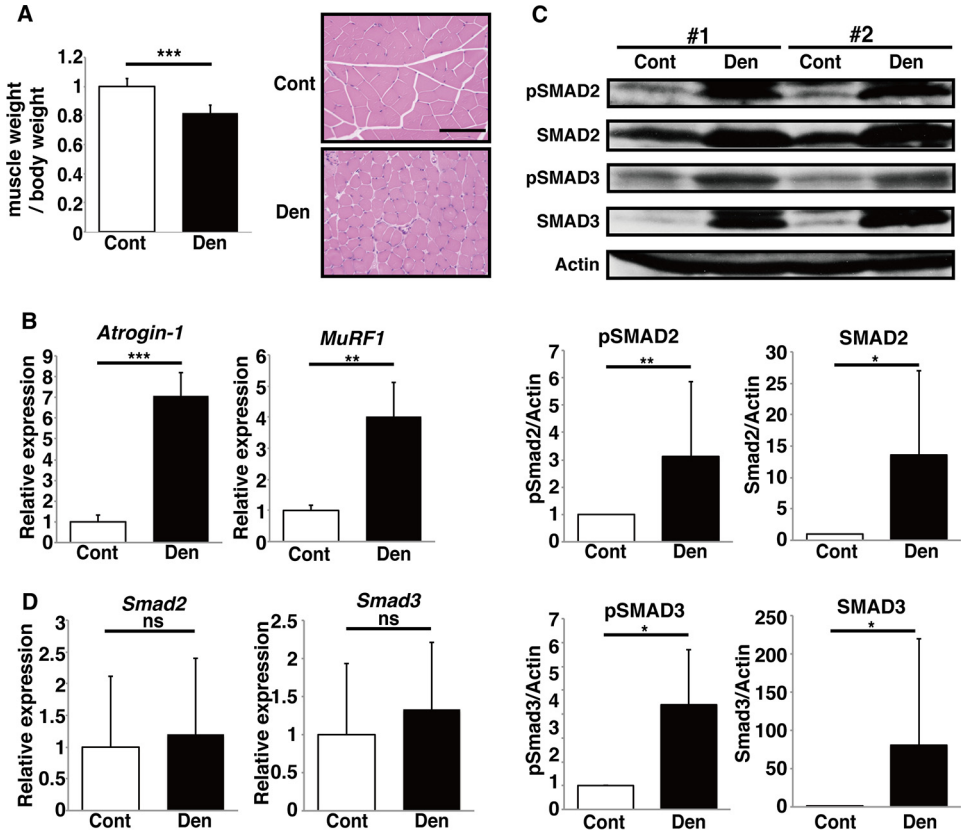

FIGURE 1. **Smad2 and Smad3 proteins accumulate in denervation-induced immobilized atrophic muscle.** *A–D,* hemi-sciatic nerve denervation-induced immobilized muscle atrophy was established in gastrocnemius muscle of wild-type mice, and muscle weight (*A, left*), and histology (*A, right*) were compared between atrophic (*Den*) and sham-operated non-atrophic control (*Cont*) muscles. Expression of *Atrogin-1*, *MuRF1*, *Smad2,* and *Smad3* mRNAs relative to β-actin were analyzed by real time PCR (*B* and *D*), whereas phosphorylated and non-phosphorylated forms of Smad2 and Smad3 protein were examined by Western blot (*C*). Data (*A, B,* and *D*) represent mean values of the indicated parameter ± S.D. (**, $p < 0.01$; ***, $p < 0.001$; *ns*, not significant; $n = 4$ or 5). Fold-change in Smad2 and Smad3 protein levels between atrophic and control muscle are shown as mean Smad2 or Smad3/actin signal intensity ± S.D. (*C*, *, $p < 0.05$; **, $p < 0.01$; ***, $p < 0.001$; *ns*, not significant; $n = 4$ or 5). Two independent data sets *(#1* and *#2*) are shown (*C*).

Immunohistochemistry—Harvested muscle was fixed in 10% neutral buffered formalin, embedded in paraffin, and cut into 4-μm sections. After microwave treatment for 10 min in 1 mM EDTA (pH 6.0) for antigen retrieval and blocking with 5% BSA/PBS for 60 min, sections were stained with anti-IGF1 receptor β (9750, 1:1600 dilution; Cell Signaling) overnight at 4 °C. After washing in PBS, sections were stained with Alexa Fluor 488/goat anti-rabbit IgG (1:100 dilution; Invitrogen) for 1 h at room temperature. DAPI (1:2000; Wako Pure Chemicals Industries, Osaka, Japan) served as a nuclear stain. Sections were examined using fluorescence microscopy (Biorevo; Keyence, Osaka, Japan).

Metabolome Analysis—Frozen tissue (~40 mg) was added to methanol (500 μl) containing internal standards (20 μmol/liter each of methionine sulfone and D-camphor-10-sulfonic acid) and homogenized using a cell disrupter. Then chloroform (500 μl) and Milli-Q water (200 μl) were added to the homogenate. The solution was thoroughly mixed and then centrifuged at 4600 × *g* for 15 min at 4 °C, and the aqueous fraction was centrifugally filtered through a Millipore 5-kDa cutoff filter to remove large molecules. The filtrate was dried using an evacuated centrifuge and dissolved in Milli-Q water (50 μl) containing 200 μmol/liter reference compounds (3-aminopyrrolidine and trimesic acid) prior to capillary electrophoresis/mass spectrometry analysis. Capillary electrophoresis/mass spectrometry-based metabolomic profiling and data analysis were performed essentially as described (32–36).

Statistical Analysis—Statistical analysis was performed using the unpaired two-tailed.

Student's *t* test (*, $p < 0.05$; **, $p < 0.01$; ***, $p < 0.001$; *NS* means not significant, throughout the paper). All data are expressed as means ± S.D.

Results

Smad2/3 Protein Accumulates in Atrophic Muscle—Because immobilization-induced skeletal muscle atrophy occurs only in directly affected muscle, we hypothesized that atrophic signals are regulated cell-intrinsically rather than systemically. Thus, we examined changes in levels of intracellular proteins in skeletal muscle following unilateral sciatic nerve denervation in 8-week-old mice. Significantly reduced skeletal muscle volume was evident in gastrocnemius muscle 1 week after denervation compared with the sham-operated side (Fig. 1*A*), and expression of mRNAs encoding atrophy-associated ubiquitin ligases such as *Atrogin-1* and *MuRF1* increased in atrophic muscle compared with non-atrophic muscle (Fig. 1*B*). Western analysis showed that Smad2/3 proteins, which are downstream effectors of myostatin-ActRIIB signaling, accumulated significantly in atrophic muscle (Fig. 1*C*). The fact that our model enables comparison between denervation-induced atrophic and sham-

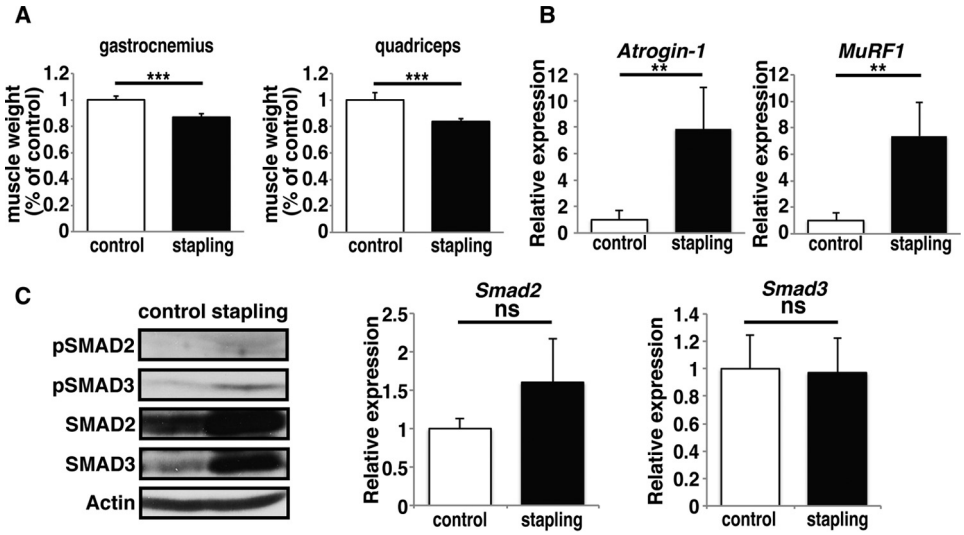

FIGURE 2. **Smad2 and Smad3 accumulate at protein but not mRNA levels in fixation-induced immobilized atrophic muscle.** *A–C,* muscle atrophy caused by fixation using a stapling procedure (*stapling*) was generated in the left lower extremity of wild-type mice, and weight of gastrocnemius or quadriceps muscle (*A*), or expression of *Atrogin-1*, *MuRF1*, *Smad2*, or *Smad3* mRNAs relative to β-actin (*B* and *C*), and expression of Smad2, Smad3, pSmad2, and pSmad3 proteins in gastrocnemius was examined (*C*). Data (*A–C*) represent mean values of indicated parameters ± S.D. (**, $p < 0.01$; ***, $p < 0.001$; *ns,* not significant; $n = 5$).

operated non-atrophic muscle in the same mouse meant that levels of circulating factors were comparable, supporting the idea that Smad2/3 accumulation in atrophic muscle is regulated cell-intrinsically. Furthermore, neither *Smad2* nor *Smad 3* mRNA levels were up-regulated in atrophic compared with non-atrophic muscle (Fig. 1*D*). Nerve activity may function to maintain muscle homeostasis; however, accumulation of both total Smad2/3 and phospho (pSmad2/3)-protein in the absence of mRNA up-regulation was also seen in a different immobilization-induced model (a fixation model) without denervation (Fig. 2), suggesting that Smad2/3 accumulation is a universal mechanism underlying immobilization-induced muscle atrophy. Thus, we utilized the denervation model for the following *in vivo* immobilization-induced muscle atrophy model.

Smad2/3 Protein Accumulation Is Required for Skeletal Muscle Atrophy—To determine how Smad2/3 protein accumulation functions in skeletal muscle atrophy, we generated skeletal muscle-specific Smad2/3 doubly deficient (DKO) mice by crossing *Smad2*$^{flox/flox}$/Smad3 null mice with creatine kinase muscle Cre mice (Fig. 3*A*). *Smad2* mRNA expression was significantly down-regulated in DKO mice (data not shown). Interestingly, Smad2/3 DKO mice were resistant to denervation-induced muscle atrophy shown by reduced muscle weight and CSA of fibers. These observations support the idea that Smad2/3 proteins are required for muscle atrophy (Fig. 3, *B* and *C*). Significant up-regulation of *Atrogin-1* and *MuRF1* expression seen in atrophic relative to control non-atrophic muscles was not evident in Smad2/3 DKO mice (Fig. 3*D*), supporting the idea that Smad2/3 protein accumulation is required for both atrophy of immobilized muscle and atrogene expression. The bone morphogenetic protein-Smad1/5/8 axis is reportedly activated by BMP7 to promote muscle hypertrophy (37), and Smad1/5/8 are required for myostatin-induced muscle hypertrophy (38). Indeed, we detected Smad1/5/8 activation in muscle of WT, Smad2 cKO, and Smad3 KO mice following denervation; however, Smad1/5/8 activation was less robust in DKO than other mice (Fig. 3*E*). Akt protein accumulated following loss of either Smad2 or Smad3 in denervated muscle (Fig. 3*E*). This finding suggests that hypertrophic signals via Smad1/5/8 are activated following denervation and are Smad2/3-dependent mechanisms.

Myostatin Is Dispensable for Smad2/3 Protein Accumulation and Skeletal Muscle Atrophy—Mice deficient in myostatin exhibit elevated muscle volume (28), and anti-myostatin or anti-ActRIIB antibodies have been developed as human therapies for muscle atrophy (27). Smad2/3 is reportedly activated following myostatin stimulation. To analyze how changes in myostatin expression might affect skeletal muscle atrophy in adult animals, we generated global but inducible myostatin knock-out mice by crossing myostatin$^{flox/flox}$ mice with interferon-inducible Mx-1 promoter-driven Cre (Mx-Cre) mice (Mstn cKO; Mx;myostatin$^{flox/flox}$). Myostatin cKO was induced at 8 weeks of age, and then denervation was performed. Following unilateral denervation, we observed denervation-induced muscle atrophy in both Mstn cKO and control mice (Fig. 4*A*). In addition, pSmad2/3 and Smad2/3 total protein accumulation in atrophic relative to non-atrophic muscle occurred in both Mstn cKO and control mice (Fig. 4*B*). Expression of both *Atrogin-1* and *MuRF1* significantly increased in atrophic compared with non-atrophic muscle of Mstn cKO and control mice following denervation (Fig. 4*C*), suggesting that myostatin is dispensable for immobilization-induced pSmad2/3 and total Smad2/3 protein accumulation and skeletal muscle atrophy.

IGF1 Signals Block Smad2/3 Protein Accumulation in Muscle—Next we employed serum starvation of C2C12 myogenic cells, an *in vitro* muscle atrophy model (39), to examine Smad2/3 effects *in vitro*. Serum-starved C2C12 cells showed Smad2/3 accumulation at protein but not mRNA levels as well as elevated expression of *Atrogin-1* and *MuRF1,* effects seen *in vivo* (Fig. 5, *A* and *B*). Serum starvation conditions differ from immobilization; however, we utilized this model because Smad2/3 protein but not mRNA accumulation occurred concomitantly with the elevated *Atrogin-1* and *MuRF1* levels in myogenic cells *in vitro* as observed *in vivo* immobilization mod-

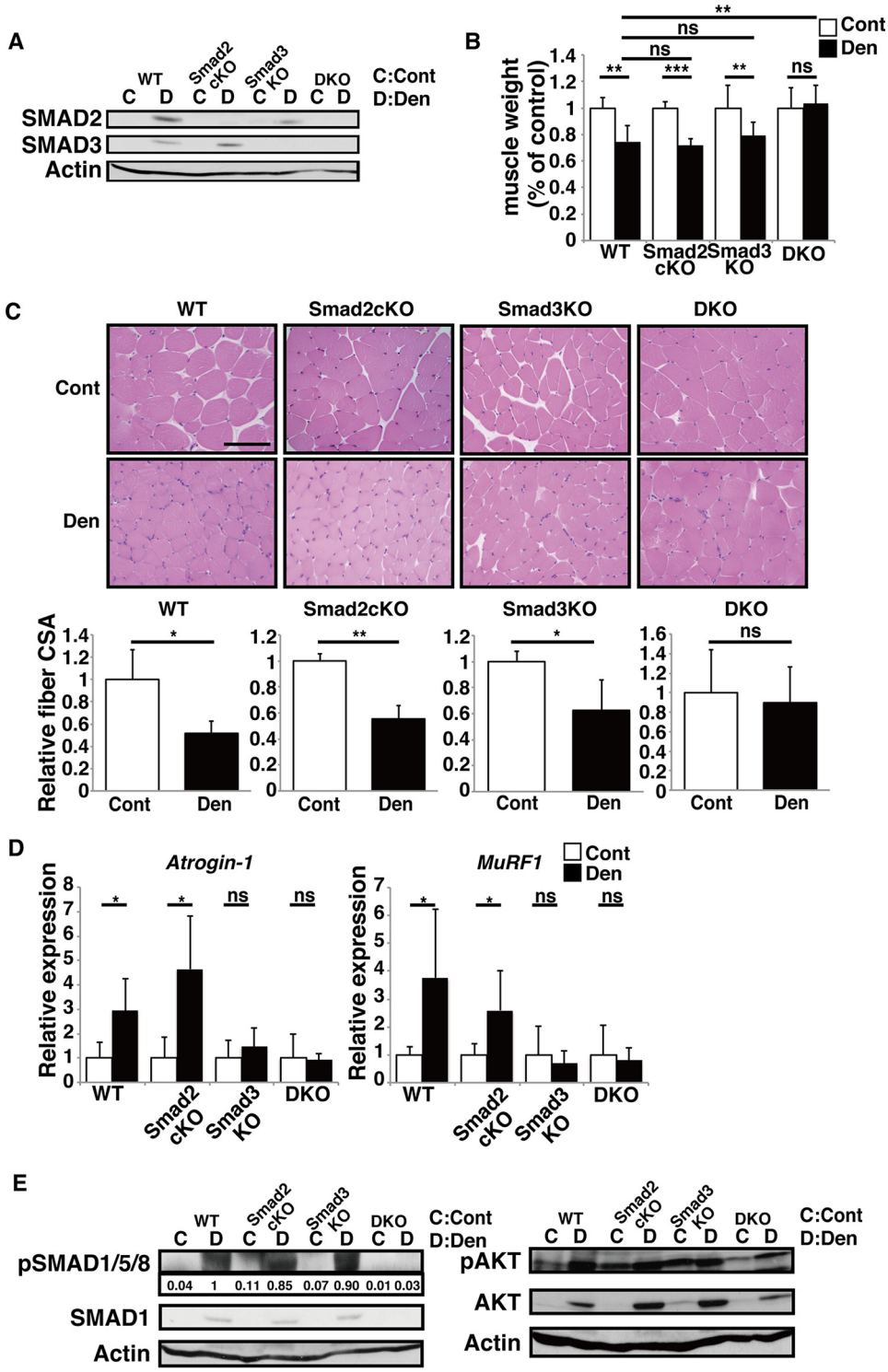

FIGURE 3. **Smad2/3 are required for denervation-induced muscle atrophy.** *A–E,* hemi-sciatic nerve denervation-induced muscle atrophy was generated in gastrocnemius muscle of wild-type (*WT*), Smad2 cKO, Smad3 KO, and Smad2/3 DKO mice. Smad2, Smad3, pSmad2, pSmad3, pSmad1/5/8, Smad1, pAkt, Akt, and actin expression was determined by Western blot (*A* and *E*). Shown are muscle weight (*B*), histology and CSA of muscle fiber based on H&E staining (*C*), and real time PCR analysis of *Atrogin-1* and *MuRF1* mRNAs relative to β-actin (*D*), in denervated (*Den*) *versus* control (*Cont*) sides. Data (*B–D*) represent mean values of the indicated parameter ± S.D. (*, $p < 0.05$; **, $p < 0.01$; ***, $p < 0.001$; *ns,* not significant; $n = 5–11$). Levels of immunoblotted pSmad1/5/8 proteins relative to actin were quantified (*E*).

els. Elevated *Atrogin-1* and *MuRF1* expression in serum-starved C2C12 cells was significantly inhibited by addition of exogenous IGF1, which promotes anabolic signaling in muscle (40, 41), or SIS3, a Smad3 inhibitor (Fig. 5*B*). SIS3 treatment did not elevate Akt activity in serum-starved C2C12 cells (data not shown). IGF1 effects were abolished by treatment of cells with either LY294002, an Akt inhibitor, or U0126, a MEK (and thus ERK) inhibitor (Fig. 5*C*). Akt activation by IGF1 in C2C12 cells was unchanged by either SIS3 or U0126 treatment (Fig. 5*D*). IGF1 treatment also blocked Smad2/3 protein accumulation

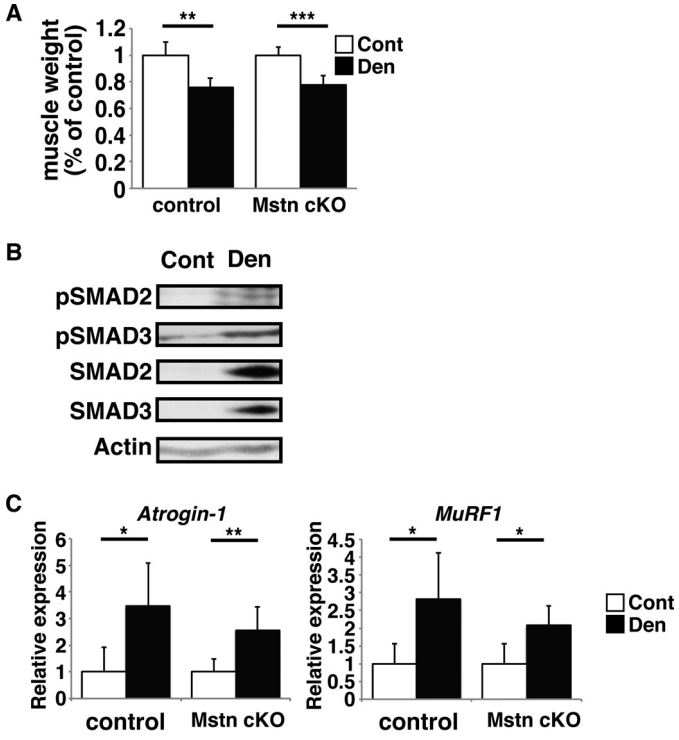

FIGURE 4. **Myostatin is dispensable for denervation-induced muscle atrophy and Smad2/3 protein accumulation.** *A–C,* control (*control*) and Mstn cKO (*cKO*) mice were generated, and hemi-sciatic nerve denervation-induced muscle atrophy was generated in gastrocnemius muscle of mice of both genotypes. Shown are muscle weight (*A*), Smad2, Smad3, pSmad2, and pSmad3 protein levels based on immunoblotting (*B*), and real time PCR analysis of *Atrogin-1* and *MuRF1* mRNAs relative to β-actin analyzed (*C*), in muscles of denervated (*Den*) and control (*Cont*) sides. Data (*A* and *C*) represent mean values of the indicated parameter ± S.D. (*, $p < 0.05$; **, $p < 0.01$; ***, $p < 0.001$; *ns,* not significant; $n = 5$).

in serum-starved C2C12 cells, an effect reversed by either LY294002 or U0126 treatment (Fig. 5*E*). Interestingly, the ability of IGF1 to block starvation-induced Smad2/3 protein accumulation was abolished by treating cells with the proteasome inhibitor MG132 (Fig. 5*F*), suggesting that Smad2/3 proteins are regulated at steady state by the ubiquitin/proteasome pathway in skeletal muscle and that IGF1 loss promotes Smad2/3 protein stabilization and concomitant accumulation followed by skeletal muscle atrophy.

IGF1 Receptor Activation Is Abrogated by Muscle Immobilization—Next, we asked how muscle immobilization impairs IGF1 signaling. Recently, the E3 ubiquitin ligases Cbl-b or Fbxo40 were shown to play a crucial role in inducing muscle atrophy by degrading IRS1, an IGF1 signal transducer (10, 42). However, we did not detect significant elevation of mRNAs encoding either factor in atrophic compared with non-atrophic muscle in our immobilization-induced atrophy models (data not shown). Interestingly, however, IGF1 receptor phosphorylation, as analyzed by Western blot, decreased in denervation-induced atrophic compared with non-atrophic muscle (Fig. 6*A*), and comparable changes were seen in fixation-induced atrophic muscle (data not shown). It is noteworthy that in this experimental system impaired IGF1 receptor activation occurs only atrophic muscle, despite the fact that both atrophic and non-atrophic muscle are exposed to equivalent levels of circulating IGF1. We, in fact, confirmed that denervated and sham-operated mice showed similar levels of circulating IGF1 (Fig. 6*B*).

Finally, we evaluated potential metabolic changes underlying muscle atrophy. Like insulin, IGF1 promotes cellular glucose uptake (43–45). Given that IGF1 receptor phosphorylation (and hence activation) is impaired in atrophic muscle, we analyzed glucose levels in immobilized muscle and found that they were significantly lower in denervation-induced atrophic than in sham-operated non-atrophic muscle (Fig. 6*C*). Lower glucose levels were accompanied by lower ATP levels in atrophic compared with non-atrophic muscle (Fig. 6*C*). By contrast, levels of the BCAAs leucine, isoleucine, and valine were significantly elevated in atrophic *versus* non-atrophic muscle (Fig. 6*D*), an effect indicative of protein degradation. Reduced glucose uptake into muscle was also seen in *Smad2/3* DKO denervated relative to non-denervated muscles following denervation (Fig. 6*E*), although elevation of BCAA production in muscles by denervation was altered in DKO mice (Fig. 6*F*). These results suggest that muscle atrophy is accompanied by altered energy homeostasis.

Discussion

Skeletal muscle volume is controlled by a balance of anabolic and catabolic signals (1, 2). Thus, decreased muscle volume occurs via either down-regulated anabolic signals, which occur in conditions such as starvation or elevated catabolic signals, which are activated by prolonged inactivity, limb fixation, muscle disuse, steroid use, or mechanical unloading (3). Here, we found that muscle immobilization by either denervation or limb fixation impairs IGF1 receptor activation based on observed changes in phosphorylation levels, followed by accumulation of Smad2/3 proteins (Fig. 6*G*). Because we detected phosphorylation of Smad2 and Smad3 in muscle after immobilization by either denervation or fixation, we conclude that activation and accumulation of Smad2/3 protein is required for muscle atrophy. Smad2/3 protein phosphorylation was detected in muscle following denervation even in myostatin cKO mice (Fig. 4*B*). Thus, further studies are needed to identify activators upstream of Smad2/3 after muscle immobilization. Interestingly, IGF1 receptor activation was inhibited specifically in atrophic but not in non-atrophic muscles in the same animal, in the presence of comparable levels of circulating IGF1 ligand. This finding means that muscle atrophy seen in immobilized muscle is not driven systemically. Smad2/3 are reported downstream effectors of myostatin-ActRIIB signaling (46); however, we found that myostatin was dispensable for immobilization-induced Smad2/3 activation. By contrast, lack of Smad2/3 in muscles resulted in significant resistance to immobilization-induced skeletal muscle atrophy and induced atrogene expression. These results suggest that Smad2/3 protein accumulation is regulated cell intrinsically via a localized mechanism rather than systemically.

We also show that muscle atrophy is closely related to energy metabolism and that BCAA generation accompanied by muscle atrophy is Smad2/3-dependent. Because BCAA cannot be synthesized *de novo*, elevated BCAA levels in atrophic muscles are likely due to Smad2/3-dependent protein degradation. Overall,

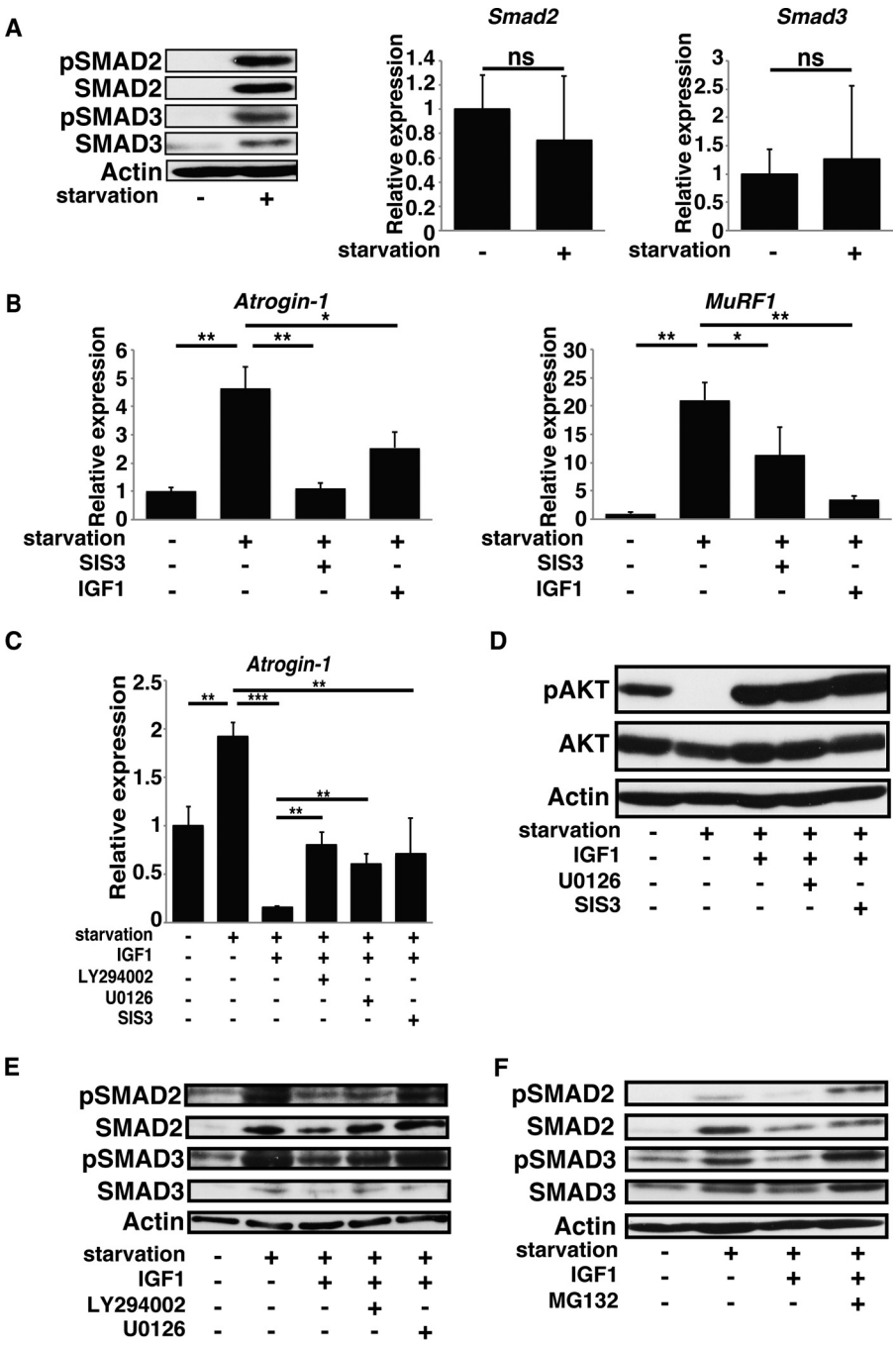

FIGURE 5. **IGF1 regulates Smad2/3 protein accumulation in C2C12 myogenic cells.** *A–F,* C2C12 myogenic cells were cultured in DMEM supplemented with (*starvation* −) or without (*starvation* +) 10% FCS in the presence or absence of indicated factors (100 ng/ml IGF1; 10 μM SIS3, a Smad3 inhibitor; 10 μM LY294002, an AKT inhibitor; 10 μM U0126, a MEK (ERK) inhibitor; or 10 μM MG132, a proteasome inhibitor). pSmad2, pSmad3, Smad2, Smad3, pAkt, Akt, and actin proteins were analyzed by Western blot, and *Smad2*, *Smad3*, *Atrogin-1,* or *MuRF1* mRNAs relative to β-actin were analyzed by real time PCR. Data (*A–C*) represent mean *Smad2*, *Smad3*, *Atrogin-1,* or *MuRF1* expression relative to β-actin ± S.D. (*, $p < 0.05$; **, $p < 0.01$; ***, $p < 0.001$; *ns,* not significant; $n = 5$).

our study suggests that Smad2/3 could be considered potential therapeutic targets to prevent skeletal muscle atrophy.

IGF1 signaling in muscle reportedly inhibits muscle atrophy through Akt-dependent phosphorylation and cytosolic sequestration of FOXOs, which are upstream activators of atrophy-related genes (7, 12). One of those atrophy-related genes, the ubiquitin ligase Cbl-b, is required to promote unloading-induced atrophy by inhibiting IGF1 signaling via ubiquitinating and destabilizing IRS1, an IGF1 signal transducer, and activating FoxO3 (10). Thus, in a muscle atrophy model, IGF1 signaling is impaired at the signal transducer level. However, in our immobilization-induced muscle atrophy models, we did not detect significant activation of *Cbl-b* expression in atrophic muscle (data not shown) but rather observed impaired IGF1 signaling at the receptor level, even under normal circulating IGF1 concentrations. We also showed that IGF1 signals suppress Smad2/3 protein accumulation following serum starvation in C2C12 cells, effects rescued by treatment with Akt or ERK inhibitors or with the proteasome inhibitor MG132. These results suggest that muscle movement may activate the Akt,

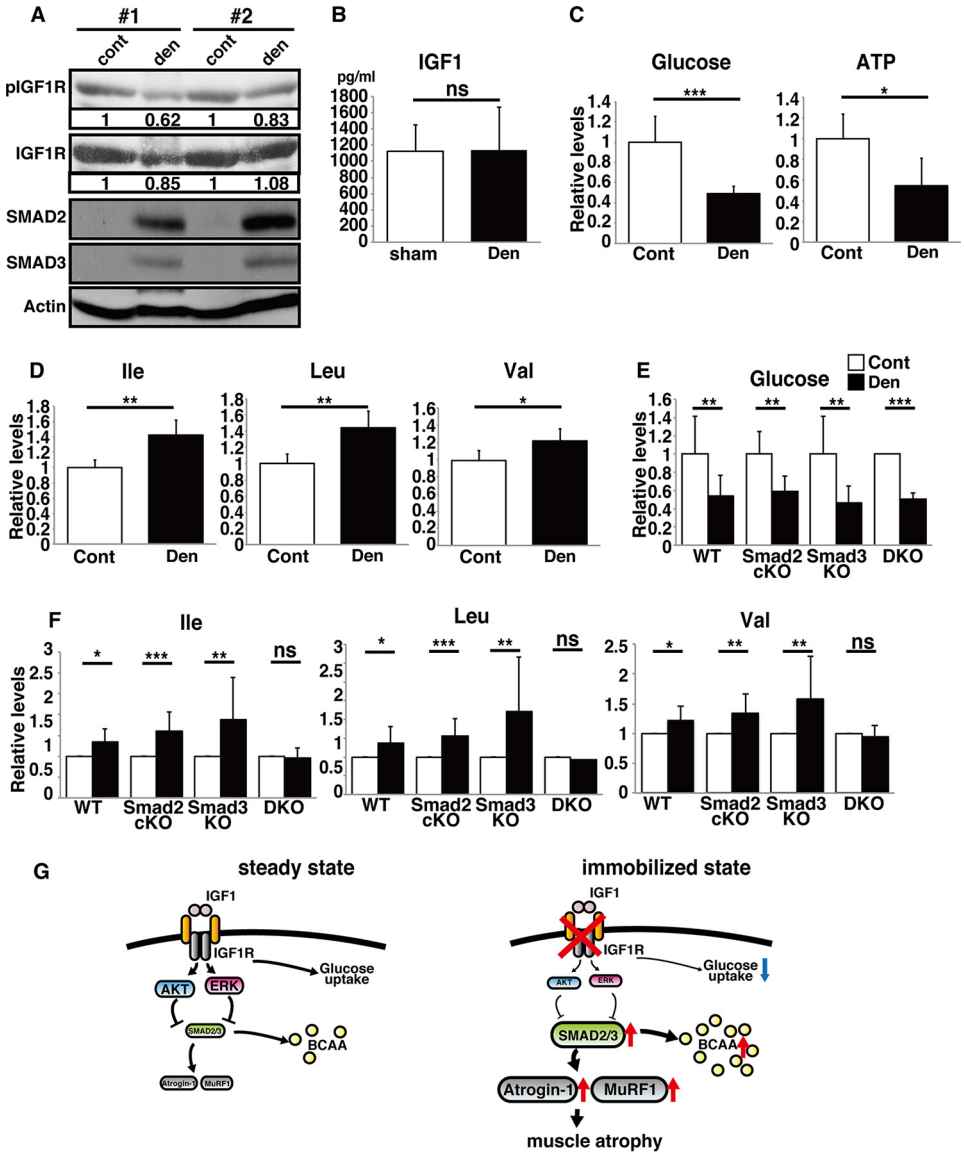

FIGURE 6. **Atrophic muscle exhibits IGF1R deactivation and elevated BCAA levels.** *A* and *C*, hemi-sciatic nerve denervation-induced muscle atrophy was generated in gastrocnemius muscle of wild-type (*WT*), Smad2 cKO, Smad3 KO, or Smad2/3 DKO mice. Indicated proteins were analyzed by Western blotting (*A*), and levels of glucose, ATP, and BCAAs (isoleucine (*Ile*), leucine (*Leu*), and valine (*Val*)) were compared between denervated atrophic (*Den*) and sham-operated non-atrophic control (*Cont*) sides (*C–F*). All data are means ± S.D. ($n = 7$). *, $p < 0.05$; **, $p < 0.01$; ***, $p < 0.005$; *ns*, not significant. Levels of immunoblotted pIGF1R or IGF1R proteins relative to actin were quantified (*A*). *B,* bilateral sciatic nerve denervation (*Den*) or sham surgery (*sham*) was performed in wild-type mice, and serum IGF1 levels in each group were analyzed by ELISA. Data represent mean serum IGF1 concentration ± S.D. (*ns,* not significant; $n = 4$). Two independent data sets (*#1* and *#2*) are shown (*A*). *G,* schematic model of immobilization-induced muscle atrophy. In non-immobilized conditions at steady state, muscle IGF1 receptor is activated, continuously suppressing Smad2/3 protein accumulation and inhibiting Atrogin-1/MuRF1 expression and glucose uptake (*G, left*). In immobilized conditions, muscle IGF1 receptor is de-activated, enabling Smad2/3 protein accumulation, Atrogin-1/MuRF1 expression, and resultant atrophy (*G, right*). Immobilization also inhibits glucose uptake by muscles and elevates BCAA levels.

ERK, or ubiquitin-proteasome systems to inhibit Smad2/3, IGF1-dependently.

An interesting phenomena reported here is that IGF1 receptors in immobilized muscle are insensitive to circulating IGF1 ligands, whereas IGF1 receptors in non-atrophic muscle are activated in a normal fashion, a finding consistent with the report that IGF1 overexpression in skeletal muscle does not prevent unloading-induced muscle atrophy (47). Smad2/3 protein accumulation in muscle atrophy in our models did not depend on circulating myostatin. Myostatin deficiency reportedly results in muscle hypertrophy (48), but we found that myostatin inhibition in adult animals did not increase muscle volume (data not shown). Moreover, IGF1 receptor deficiency in muscle reportedly significantly reduces muscle volume (49). These results suggest that muscle volume is likely regulated cell intrinsically in adult animals. At present, how immobilization promotes IGF1 receptor insensitivity in muscle remains unclear, but our results clearly show that muscle movement maintains IGF1 receptor activation as a means of achieving muscle homeostasis.

To date, various mechanisms underlying muscle atrophy have been reported, including elevated levels of reactive oxygen species or inflammatory cytokines or activation of glucocorticoid receptors (50–52). However, it remains unclear whether

the mechanisms identified here, namely IGF1 receptor insensitivity and Smad2/3 protein accumulation, are applicable to other types of muscle atrophy, although common mechanisms may underlie various forms of muscle atrophy. For example, the atrogenes Atrogin-1 and MuRF1 are reportedly universally up-regulated in atrophic muscle following denervation, immobilization, or unloading; furthermore, Atrogin-1 or MuRF1 deficiency promotes partial but significant resistance to denervation-induced muscle atrophy (8). Unloading also activates FoxO3, which is upstream of Atrogin-1 and MuRF1, in atrophic muscle, and Cbl-b deficiency inhibits both FoxO3 activation and Atrogin-1/MuRF1 expression in an unloading-induced muscle atrophy model (10). By contrast, in a steroid-induced muscle atrophy model, glucocorticoid receptor activity reportedly directly induces expression of KLF15, a factor required to induce Atrogin-1 and MuRF1 expression, following dexamethasone stimulation of myogenic cells (53). KLF15 knockdown blocks the ability of dexamethasone to induce Atrogin-1 and MuRF1 (53). We found that targeting Smad2/3 in muscle promoted resistance to denervation-induced muscle atrophy and inhibited Atrogin-1/MuRF1 expression. Recently, factors other than Atrogin-1/MuRF1, such as Traf6, Musa1/Fbxo30, Smart/Fbxo21, and Fbxo31, were reported to be up-regulated in denervation-induced muscle atrophy (54, 55); however, we did not detect differences in expression of those genes in muscle of control and DKO mice after denervation (data not shown). Reasons for these discrepancies remain unknown, but they could be due to differences of experimental design. For example, *Traf6* is reportedly up-regulated in tibialis anterior muscles 4 days after denervation, whereas *Musa1/Fbxo30*, *Smart/Fbxo21,* and *Fbxo31* were shown to be up-regulated 3 days after denervation in gastrocnemius muscle (54, 55). Taken together, although their activity may differ in specific contexts, activators of Atrogin-1/MuRF1 could serve as therapeutic targets to prevent the muscle atrophy.

We also found that deactivation of the IGF1 receptor by muscle immobilization significantly reduced intracellular glucose levels relative to normal muscle, possibly as an energy-saving mechanism. Dysfunctional muscle may instead act as a BCAA reservoir to drive the tricarboxylic acid cycle. Increasing levels of circulating BCAAs are also reported in steroid-induced muscle atrophy models (53). We did not detect BCAA elevation in sera following sciatic nerve denervation (data not shown), but that is likely due to the small amount of atrophic muscle compared with that seen in steroid-induced systemic atrophy. Nonetheless, BCAA generation following muscle atrophy may occur universally. Following denervation, muscle atrophy and concomitant increases in BCAA in that muscle were seen in both Smad2 cKO and Smad3 KO mice, but both were abrogated in Smad2/3 DKO mice (Fig. 6*F*). These data suggest that Smad2 and Smad3 have a redundant function in immobilization-induced muscle atrophy and BCAA production in muscle. Nonetheless, the absence of muscle atrophy plus the lack of BCAA generation seen following denervation in Smad2/3 DKO mice suggest that Smad2/3 are required for degradation of muscle proteins to BCAA in conditions of atrophy. By contrast, glucose uptake likely depends on movement-induced IGF1 receptor activation rather than Smad2/3; thus reduced glucose uptake was seen in both Smad2/3 DKO and control mice after denervation. IGF1 receptor inactivation was not evident *in vitro* in C2C12 cells, even under serum starvation conditions, and Smad2/3 accumulation in serum-starved myogenic cells was antagonized by IGF1 signaling in an Akt-dependent manner.

Today, sarcopenia is a serious health concern in the elderly. At present, there is no medicine available to block muscle weakness and deterioration, but understanding mechanisms underlying immobilization-induced muscle atrophy may shed light on "disuse"-induced, age-related muscle atrophy. Further studies are needed to elucidate whether mechanisms underlying immobilization-induced muscle atrophy described here are applicable to age-related sarcopenia in human subjects.

Author Contributions—T. T. performed and analyzed data shown in Figs. 1–6. A. H., T. S., and M. T. performed and analyzed data shown in Fig. 6. M. F. analyzed and interpreted data shown in Fig. 4. Y. S. and T. K. prepared and maintained mice analyzed in Figs. 1–6. A. F., A. K., M. Matsumoto, M. Nakamura, and Y. T. designed the study. W. H., R. W., M. Morita, T. O., and K. M. analyzed and interpreted data shown in Figs. 1–6. M. Nomura and A. Y. prepared mice and interpreted data shown in Figs. 3 and 6. T. M. designed the study and wrote the paper. All authors reviewed the results and approved the final version of the manuscript.

Acknowledgments—We thank S. Ikeda, F. Shoji, and N. Yamaguchi for technical support.

References

1. Sandri, M. (2008) Signaling in muscle atrophy and hypertrophy. *Physiology* **23,** 160–170
2. Jackman, R. W., and Kandarian, S. C. (2004) The molecular basis of skeletal muscle atrophy. *Am. J. Physiol. Cell Physiol.* **287,** C834–C843
3. Foletta, V. C., White, L. J., Larsen, A. E., Léger, B., and Russell, A. P. (2011) The role and regulation of MAFbx/atrogin-1 and MuRF1 in skeletal muscle atrophy. *Pflugers Arch.* **461,** 325–335
4. Cruz-Jentoft, A. J., Baeyens, J. P., Bauer, J. M., Boirie, Y., Cederholm, T., Landi, F., Martin, F. C., Michel, J. P., Rolland, Y., Schneider, S. M., Topinková, E., Vandewoude, M., Zamboni, M., and European Working Group on Sarcopenia in Older People (2010) Sarcopenia: European consensus on definition and diagnosis: Report of the European Working Group on Sarcopenia in Older People. *Age Ageing* **39,** 412–423
5. Bodine, S. C., Stitt, T. N., Gonzalez, M., Kline, W. O., Stover, G. L., Bauerlein, R., Zlotchenko, E., Scrimgeour, A., Lawrence, J. C., Glass, D. J., and Yancopoulos, G. D. (2001) Akt/mTOR pathway is a crucial regulator of skeletal muscle hypertrophy and can prevent muscle atrophy *in vivo*. *Nat. Cell Biol.* **3,** 1014–1019
6. Pallafacchina, G., Calabria, E., Serrano, A. L., Kalhovde, J. M., and Schiaffino, S. (2002) A protein kinase B-dependent and rapamycin-sensitive pathway controls skeletal muscle growth but not fiber type specification. *Proc. Natl. Acad. Sci. U.S.A.* **99,** 9213–9218
7. Sandri, M., Sandri, C., Gilbert, A., Skurk, C., Calabria, E., Picard, A., Walsh, K., Schiaffino, S., Lecker, S. H., and Goldberg, A. L. (2004) Foxo transcription factors induce the atrophy-related ubiquitin ligase atrogin-1 and cause skeletal muscle atrophy. *Cell* **117,** 399–412
8. Bodine, S. C., Latres, E., Baumhueter, S., Lai, V. K., Nunez, L., Clarke, B. A., Poueymirou, W. T., Panaro, F. J., Na, E., Dharmarajan, K., Pan, Z. Q., Valenzuela, D. M., DeChiara, T. M., Stitt, T. N., Yancopoulos, G. D., and Glass, D. J. (2001) Identification of ubiquitin ligases required for skeletal muscle atrophy. *Science* **294,** 1704–1708
9. Gomes, M. D., Lecker, S. H., Jagoe, R. T., Navon, A., and Goldberg, A. L. (2001) Atrogin-1, a muscle-specific F-box protein highly expressed during muscle atrophy. *Proc. Natl. Acad. Sci. U.S.A.* **98,** 14440–14445

10. Nakao, R., Hirasaka, K., Goto, J., Ishidoh, K., Yamada, C., Ohno, A., Okumura, Y., Nonaka, I., Yasutomo, K., Baldwin, K. M., Kominami, E., Higashibata, A., Nagano, K., Tanaka, K., Yasui, N., Mills, E. M., *et al.* (2009) Ubiquitin ligase Cbl-b is a negative regulator for insulin-like growth factor 1 signaling during muscle atrophy caused by unloading. *Mol. Cell. Biol.* **29,** 4798–4811
11. Lee, S. W., Dai, G., Hu, Z., Wang, X., Du, J., and Mitch, W. E. (2004) Regulation of muscle protein degradation: coordinated control of apoptotic and ubiquitin-proteasome systems by phosphatidylinositol 3-kinase. *J. Am. Soc. Nephrol.* **15,** 1537–1545
12. Stitt, T. N., Drujan, D., Clarke, B. A., Panaro, F., Timofeyva, Y., Kline, W. O., Gonzalez, M., Yancopoulos, G. D., and Glass, D. J. (2004) The IGF-1/PI3K/Akt pathway prevents expression of muscle atrophy-induced ubiquitin ligases by inhibiting FOXO transcription factors. *Mol. Cell* **14,** 395–403
13. Tintignac, L. A., Lagirand, J., Batonnet, S., Sirri, V., Leibovitch, M. P., and Leibovitch, S. A. (2005) Degradation of MyoD mediated by the SCF (MAFbx) ubiquitin ligase. *J. Biol. Chem.* **280,** 2847–2856
14. Li, H. H., Kedar, V., Zhang, C., McDonough, H., Arya, R., Wang, D. Z., and Patterson, C. (2004) Atrogin-1/muscle atrophy F-box inhibits calcineurin-dependent cardiac hypertrophy by participating in an SCF ubiquitin ligase complex. *J. Clin. Invest.* **114,** 1058–1071
15. Kedar, V., McDonough, H., Arya, R., Li, H. H., Rockman, H. A., and Patterson, C. (2004) Muscle-specific RING finger 1 is a *bona fide* ubiquitin ligase that degrades cardiac troponin I. *Proc. Natl. Acad. Sci. U.S.A.* **101,** 18135–18140
16. Lagirand-Cantaloube, J., Offner, N., Csibi, A., Leibovitch, M. P., Batonnet-Pichon, S., Tintignac, L. A., Segura, C. T., and Leibovitch, S. A. (2008) The initiation factor eIF3-f is a major target for Atrogin-1/MAFbx function in skeletal muscle atrophy. *EMBO J.* **27,** 1266–1276
17. Jogo, M., Shiraishi, S., and Tamura, T. A. (2009) Identification of MAFbx as a myogenin-engaged F-box protein in SCF ubiquitin ligase. *FEBS Lett.* **583,** 2715–2719
18. Cohen, S., Brault, J. J., Gygi, S. P., Glass, D. J., Valenzuela, D. M., Gartner, C., Latres, E., and Goldberg, A. L. (2009) During muscle atrophy, thick, but not thin, filament components are degraded by MuRF1-dependent ubiquitylation. *J. Cell Biol.* **185,** 1083–1095
19. Fielitz, J., Kim, M. S., Shelton, J. M., Latif, S., Spencer, J. A., Glass, D. J., Richardson, J. A., Bassel-Duby, R., and Olson, E. N. (2007) Myosin accumulation and striated muscle myopathy result from the loss of muscle RING finger 1 and 3. *J. Clin. Invest.* **117,** 2486–2495
20. Späte, U., and Schulze, P. C. (2004) Proinflammatory cytokines and skeletal muscle. *Curr. Opin. Clin. Nutr. Metab. Care* **7,** 265–269
21. Reid, M. B., and Li, Y. P. (2001) Tumor necrosis factor-α and muscle wasting: a cellular perspective. *Respir. Res.* **2,** 269–272
22. Clop, A., Marcq, F., Takeda, H., Pirottin, D., Tordoir, X., Bibé, B., Bouix, J., Caiment, F., Elsen, J. M., Eychenne, F., Larzul, C., Laville, E., Meish, F., Milenkovic, D., Tobin, J., Charlier, C., and Georges, M. (2006) A mutation creating a potential illegitimate microRNA target site in the myostatin gene affects muscularity in sheep. *Nat. Genet.* **38,** 813–818
23. McPherron, A. C., and Lee, S. J. (1997) Double muscling in cattle due to mutations in the myostatin gene. *Proc. Natl. Acad. Sci. U.S.A.* **94,** 12457–12461
24. Schuelke, M., Wagner, K. R., Stolz, L. E., Hübner, C., Riebel, T., Kömen, W., Braun, T., Tobin, J. F., and Lee, S. J. (2004) Myostatin mutation associated with gross muscle hypertrophy in a child. *N. Engl. J. Med.* **350,** 2682–2688
25. Gallot, Y. S., Durieux, A. C., Castells, J., Desgeorges, M. M., Vernus, B., Plantureux, L., Rémond, D., Jahnke, V. E., Lefai, E., Dardevet, D., Nemoz, G., Schaeffer, L., Bonnieu, A., and Freyssenet, D. G. (2014) Myostatin gene inactivation prevents skeletal muscle wasting in cancer. *Cancer Res.* **74,** 7344–7356
26. Pistilli, E. E., Bogdanovich, S., Goncalves, M. D., Ahima, R. S., Lachey, J., Seehra, J., and Khurana, T. (2011) Targeting the activin type IIB receptor to improve muscle mass and function in the mdx mouse model of Duchenne muscular dystrophy. *Am. J. Pathol.* **178,** 1287–1297
27. Smith, R. C., and Lin, B. K. (2013) Myostatin inhibitors as therapies for muscle wasting associated with cancer and other disorders. *Curr. Opin. Support. Palliat. Care* **7,** 352–360
28. Trendelenburg, A. U., Meyer, A., Rohner, D., Boyle, J., Hatakeyama, S., and Glass, D. J. (2009) Myostatin reduces Akt/TORC1/p70S6K signaling, inhibiting myoblast differentiation and myotube size. *Am. J. Physiol. Cell Physiol.* **296,** C1258–C1270
29. Miyamoto, H., Katsuyama, E., Miyauchi, Y., Hoshi, H., Miyamoto, K., Sato, Y., Kobayashi, T., Iwasaki, R., Yoshida, S., Mori, T., Kanagawa, H., Fujie, A., Hao, W., Morioka, H., Matsumoto, M., *et al.* (2012) An essential role for STAT6-STAT1 protein signaling in promoting macrophage cell-cell fusion. *J. Biol. Chem.* **287,** 32479–32484
30. Miyauchi, Y., Sato, Y., Kobayashi, T., Yoshida, S., Mori, T., Kanagawa, H., Katsuyama, E., Fujie, A., Hao, W., Miyamoto, K., Tando, T., Morioka, H., Matsumoto, M., Chambon, P., Johnson, R. S., *et al.* (2013) HIF1α is required for osteoclast activation by estrogen deficiency in postmenopausal osteoporosis. *Proc. Natl. Acad. Sci. U.S.A.* **110,** 16568–16573
31. Katsuyama, E., Miyamoto, H., Kobayashi, T., Sato, Y., Hao, W., Kanagawa, H., Fujie, A., Tando, T., Watanabe, R., Morita, M., Miyamoto, K., Niki, Y., Morioka, H., Matsumoto, M., Toyama, Y., and Miyamoto, T. (2015) Interleukin-1 receptor-associated kinase-4 (IRAK4) promotes inflammatory osteolysis by activating osteoclasts and inhibiting formation of foreign body giant cells. *J. Biol. Chem.* **290,** 716–726
32. Soga, T., Igarashi, K., Ito, C., Mizobuchi, K., Zimmermann, H. P., and Tomita, M. (2009) Metabolomic profiling of anionic metabolites by capillary electrophoresis mass spectrometry. *Anal. Chem.* **81,** 6165–6174
33. Soga, T., and Heiger, D. N. (2000) Amino acid analysis by capillary electrophoresis electrospray ionization mass spectrometry. *Anal. Chem.* **72,** 1236–1241
34. Klampfl, C. W., and Buchberger, W. (2001) Determination of carbohydrates by capillary electrophoresis with electrospray-mass spectrometric detection. *Electrophoresis* **22,** 2737–2742
35. Hirayama, A., Kami, K., Sugimoto, M., Sugawara, M., Toki, N., Onozuka, H., Kinoshita, T., Saito, N., Ochiai, A., Tomita, M., Esumi, H., and Soga, T. (2009) Quantitative metabolome profiling of colon and stomach cancer microenvironment by capillary electrophoresis time-of-flight mass spectrometry. *Cancer Res.* **69,** 4918–4925
36. Sugimoto, M., Wong, D. T., Hirayama, A., Soga, T., and Tomita, M. (2010) Capillary electrophoresis mass spectrometry-based saliva metabolomics identified oral, breast and pancreatic cancer-specific profiles. *Metabolomics* **6,** 78–95
37. Winbanks, C. E., Chen, J. L., Qian, H., Liu, Y., Bernardo, B. C., Beyer, C., Watt, K. I., Thomson, R. E., Connor, T., Turner, B. J., McMullen, J. R., Larsson, L., McGee, S. L., Harrison, C. A., and Gregorevic, P. (2013) The bone morphogenetic protein axis is a positive regulator of skeletal muscle mass. *J. Cell Biol.* **203,** 345–357
38. Sartori, R., Schirwis, E., Blaauw, B., Bortolanza, S., Zhao, J., Enzo, E., Stantzou, A., Mouisel, E., Toniolo, L., Ferry, A., Stricker, S., Goldberg, A. L., Dupont, S., Piccolo, S., Amthor, H., and Sandri, M. (2013) BMP signaling controls muscle mass. *Nat. Genet.* **45,** 1309–1318
39. Stevenson, E. J., Koncarevic, A., Giresi, P. G., Jackman, R. W., and Kandarian, S. C. (2005) Transcriptional profile of a myotube starvation model of atrophy. *J. Appl. Physiol.* **98,** 1396–1406
40. Musarò, A., McCullagh, K., Paul, A., Houghton, L., Dobrowolny, G., Molinaro, M., Barton, E. R., Sweeney, H. L., and Rosenthal, N. (2001) Localized IGF-1 transgene expression sustains hypertrophy and regeneration in senescent skeletal muscle. *Nat. Genet.* **27,** 195–200
41. Alzghoul, M. B., Gerrard, D., Watkins, B. A., and Hannon, K. (2004) Ectopic expression of IGF-I and Shh by skeletal muscle inhibits disuse-mediated skeletal muscle atrophy and bone osteopenia *in vivo*. *FASEB J.* **18,** 221–223
42. Shi, J., Luo, L., Eash, J., Ibebunjo, C., and Glass, D. J. (2011) The SCF-Fbxo40 complex induces IRS1 ubiquitination in skeletal muscle, limiting IGF1 signaling. *Dev. Cell* **21,** 835–847
43. Bilan, P. J., Mitsumoto, Y., Ramlal, T., and Klip, A. (1992) Acute and long-term effects of insulin-like growth factor I on glucose transporters in muscle cells. Translocation and biosynthesis. *FEBS Lett.* **298,** 285–290
44. Dimitriadis, G., Parry-Billings, M., Dunger, D., Bevan, S., Colquhoun, A., Taylor, A., Calder, P., Krause, U., Wegener, G., and Newsholme, E. A. (1992) Effects of *in vivo* administration of insulin-like growth factor-I on

the rate of glucose utilization in the soleus muscle of the rat. *J. Endocrinol.* **133,** 37–43
45. Dimitriadis, G., Parry-Billings, M., Bevan, S., Dunger, D., Piva, T., Krause, U., Wegener, G., and Newsholme, E. A. (1992) Effects of insulin-like growth factor I on the rates of glucose transport and utilization in rat skeletal muscle *in vitro*. *Biochem. J.* **285,** 269–274
46. Sartori, R., Milan, G., Patron, M., Mammucari, C., Blaauw, B., Abraham, R., and Sandri, M. (2009) Smad2 and 3 transcription factors control muscle mass in adulthood. *Am. J. Physiol. Cell Physiol.* **296,** C1248–C1257
47. Criswell, D. S., Booth, F. W., DeMayo, F., Schwartz, R. J., Gordon, S. E., and Fiorotto, M. L. (1998) Overexpression of IGF-I in skeletal muscle of transgenic mice does not prevent unloading-induced atrophy. *Am. J. Physiol.* **275,** E373–E379
48. McPherron, A. C., Lawler, A. M., and Lee, S. J. (1997) Regulation of skeletal muscle mass in mice by a new TGF-β superfamily member. *Nature* **387,** 83–90
49. Mavalli, M. D., DiGirolamo, D. J., Fan, Y., Riddle, R. C., Campbell, K. S., van Groen, T., Frank, S. J., Sperling, M. A., Esser, K. A., Bamman, M. M., and Clemens, T. L. (2010) Distinct growth hormone receptor signaling modes regulate skeletal muscle development and insulin sensitivity in mice. *J. Clin. Invest.* **120,** 4007–4020
50. Powers, S. K., Kavazis, A. N., and DeRuisseau, K. C. (2005) Mechanisms of disuse muscle atrophy: role of oxidative stress. *Am. J. Physiol. Regul. Integr. Comp. Physiol.* **288,** R337–R344
51. Cai, D., Frantz, J. D., Tawa, N. E. Jr., Melendez, P. A., Oh, B. C., Lidov, H. G., Hasselgren, P. O., Frontera, W. R., Lee, J., Glass, D. J., and Shoelson, S. E. (2004) IKKβ/NF-κB activation causes severe muscle wasting in mice. *Cell* **119,** 285–298
52. Clarke, B. A., Drujan, D., Willis, M. S., Murphy, L. O., Corpina, R. A., Burova, E., Rakhilin, S. V., Stitt, T. N., Patterson, C., Latres, E., and Glass, D. J. (2007) The E3 Ligase MuRF1 degrades myosin heavy chain protein in dexamethasone-treated skeletal muscle. *Cell Metab.* **6,** 376–385
53. Shimizu, N., Yoshikawa, N., Ito, N., Maruyama, T., Suzuki, Y., Takeda, S., Nakae, J., Tagata, Y., Nishitani, S., Takehana, K., Sano, M., Fukuda, K., Suematsu, M., Morimoto, C., and Tanaka, H. (2011) Crosstalk between glucocorticoid receptor and nutritional sensor mTOR in skeletal muscle. *Cell Metab.* **13,** 170–182
54. Milan, G., Romanello, V., Pescatore, F., Armani, A., Paik, J. H., Frasson, L., Seydel, A., Zhao, J., Abraham, R., Goldberg, A. L., Blaauw, B., DePinho, R. A., and Sandri, M. (2015) Regulation of autophagy and the ubiquitin-proteasome system by the FoxO transcriptional network during muscle atrophy. *Nat. Commun.* **6,** 6670
55. Paul, P. K., Gupta, S. K., Bhatnagar, S., Panguluri, S. K., Darnay, B. G., Choi, Y., Kumar, A. (2010) Targeted ablation of TRAF6 inhibits skeletal muscle wasting in mice. *J. Cell Biol.* **191,** 1395–1411